ACCURATE FLUX DENSITIES AT 8·87 GHz OF 195 RADIO SOURCES

By A. J. SHIMMINS* and J. V. WALL*

[Manuscript received 6 October 1972]

Abstract

Accurate flux densities at 8·87 GHz have been determined with the Parkes 64 m telescope for 195 radio sources, using an on–off integration method. The sources were selected from the Parkes 408 and 2700 MHz catalogues as those having estimated flux densities at 8·87 GHz greater than 0·5 f.u. and relatively small angular sizes. Eighty of the selected sources are identified with QSO's, 40 with galaxies, and one with an HII region, while 74 have not been identified. The estimated accuracy of the flux density is $\pm 0 \cdot 02$ f.u. (r.m.s.) due to system noise and $\pm 3 \cdot 5\%$ due to other causes. A list of known or newly suspected radio variables in the sample is given.

I. INTRODUCTION

This paper presents accurate flux densities at 8·87 GHz ($\lambda = 3 \cdot 4$ cm) of 195 radio sources. The sources were taken from either the Parkes 408 MHz catalogue (Ekers 1969) or the currently completed parts of the new Parkes 2700 MHz catalogue (Wall *et al.* 1971; Shimmins 1971; Shimmins and Bolton 1972*b*; and unpublished Parkes data). The sources were selected as having estimated flux densities at 8·87 GHz greater than 0·5 f.u.† and angular sizes small compared with the $2' \cdot 55$ arc beam of the telescope at this frequency.

The work was undertaken partly to extend the present program of observations of spectra of radio sources to a higher frequency and partly to investigate an on–off technique for the measurement of flux densities under conditions of low signal to noise ratio.

Some of the observed sources are common to other source lists at almost the same frequency: 130 sources at 8·55 GHz by Andrievskii *et al.* (1969), 99 sources at 8·55 GHz by Gorshkov *et al.* (1970), and 60 sources at 8·00 GHz by Stull (1971). In Section VI the present measurements are compared with those of the above authors together with measurements of 146 sources at 10·63 GHz by Doherty *et al.* (1969) and 101 sources at both 6·63 and 10·7 GHz by Bell *et al.* (1971). A number of new variable sources are suggested.

II. EQUIPMENT AND OBSERVATIONS

The observations were carried out at the Parkes Observatory in a single observing session, 4–9 February 1972 (1972·10). The 64 m (210 ft) parabolic reflector was equipped with a cryogenically-cooled parametric receiver developed by the Division of Radiophysics, CSIRO. The centre frequency was 8·87 GHz, the bandwidth 30 MHz, and the system noise temperature 250 K, giving an r.m.s. noise fluctuation of 0·033 K (0·115 f.u.) for an output time constant of 2 s. A noise diode was used to produce a calibration signal of approximately 1 K (3·25 f.u.) at the receiver input.

* Division of Radiophysics, CSIRO, P.O. Box 76, Epping, N.S.W. 2121.

† 1 flux unit (f.u.) = $10^{-26}\,\mathrm{W\,m^{-2}\,Hz^{-1}}$.

The receiver was switched between two feeds, one on axis and another producing a beam 20′ arc off axis. The on-axis feed was of the two-hydrid-mode type described by Thomas (1970) and was phased to receive circular polarization. The main beam was circular, with an approximately Gaussian shape of half-power width 2′·55 arc. At high frequencies, the axial focus, lateral focus, and aperture efficiency of the telescope and also the atmospheric extinction are all functions of zenith angle. For the present observations the telescope axial focus was fixed at the optimum value for zenith angle 40° and the lateral focus at the optimum value for zenith angle 45°, while observations were made within the zenith angle range 30°–50° wherever possible.

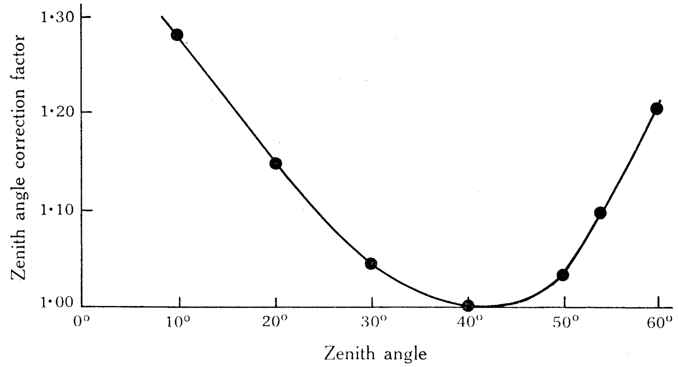

Fig. 1.—Zenith angle correction factor to compensate for changes in both atmospheric extinction and aperture efficiency and for the telescope being out of axial and lateral focus (axial focus +1·6 cm, lateral focus +4·0 cm).

The combined effects of all variations with zenith angle were determined from observations of the source PKS 0915−11 (Hydra A) over a wide range of zenith angles and from additional data supplied by D. E. Yabsley (personal communication). The zenith angle correction factor is shown in Figure 1.

In the past, measurements of flux density at high frequencies, i.e. 2·7 and 5·0 GHz, have consisted of forward and reverse scans through the position of the source in both coordinates. On-line analysis with a PDP–9 computer provided simultaneous measurement of the flux density and apparent position of the source. Corrections were subsequently applied for pointing errors (i.e. for the differences between the set and measured coordinates). The large collecting area of the telescope combined with the low system temperature and large bandwidth made possible the determination of the flux density of a source to an accuracy of 0·02 f.u. in an observing time of less than 5 min.

As the efficiency of the telescope at 8·87 GHz is somewhat lower, the receiver noise temperature some three times higher, and the bandwidth only one-tenth that of the other receivers, the use of a similar technique would have involved an increase in observing time of at least an order of magnitude. It was therefore decided to use an on–off technique in which a larger fraction of the effective observing time was spent on source. However, as the telescope pointing error, typically 0′·4 arc, is significant compared with the beamwidth, pointing corrections are larger than in the lower-frequency measurements and must be determined during the flux measurement.

The observational procedure adopted was as follows. The telescope was set approximately 5′·0 arc away from the source and the receiver sensitivity was determined by measuring the difference between the receiver output with and without the injection of a calibration signal of approximately 1 K. An integration time of 30 s was used and the measurement retained by the computer. The telescope was then

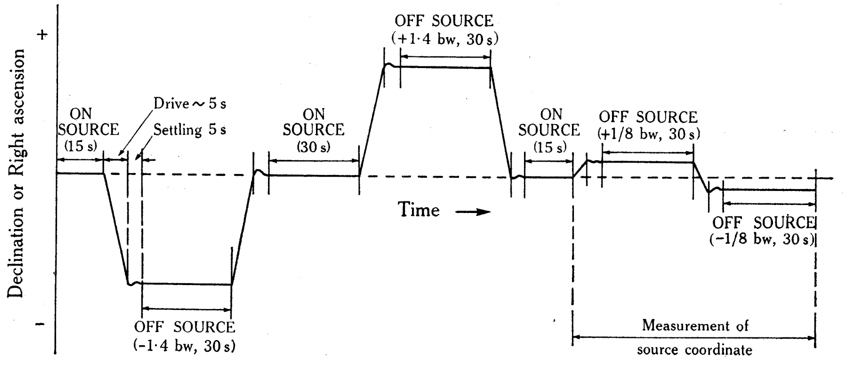

Fig. 2.—Telescope drive cycle for on–off integration series, with times in seconds and off-source locations in beamwidths (bw) as indicated.

set on the nominal position of the source and the on–off drive cycle in declination, shown in Figure 2, was initiated by the computer. At the end of the cycle the data printed out by the computer were:

(1) The values of the deflections from the on-source–off-source integrations, their mean value, and the scatter.

(2) The flux density obtained by dividing the mean value by the previous deflection due to the calibration signal and multiplying by the adopted flux equivalent of the calibration signal.

(3) The values of the deflections at $\pm 1/8$ beamwidth.

(4) Two estimates of the displacement between the set and the measured declination. These were computed from the ratio of the $\pm 1/8$ beamwidth deflections to the mean on-source deflection.

(5) The percentage correction to the flux density due to the mean of the two displacements calculated in (4).

If the value of the pointing correction was 10% or greater, i.e. the displacement in declination 30″ arc or greater, the declination cycle was repeated at an on-source declination indicated by the displacement in (4). Otherwise a new flux calibration was applied and the cycle repeated in right ascension.

For most sources satisfactory observations were obtained with one cycle in each coordinate. In a few extreme cases repeat observations were made in declination and right ascension and a further repeat in declination at the final value for the right ascension.

III. Data Reduction and Calibration

Previous flux density measurements at Parkes have been tied to the spectrum of PKS 0915−11 (Hydra A), for which a power law has been assumed. At 8·87 GHz the source is partially resolved with the 2′·55 arc beam but the structure is not sufficiently well-known to permit the calculation of an accurate size factor (which is between 1·05 and 1·10). This is because of the unknown spectrum of the halo component, which at 1425 MHz contributes 26% of the flux density and is approximately 200″ arc in diameter (Fomalont 1971). At 8·87 GHz the halo is not obvious from scans through the source and consequently its spectrum must be very steep.

The flux density scale for the present measurements was determined by comparing measured and estimated values of flux density for 10 stable small-diameter sources which have well-established power-law spectra between 1410 and 5009 MHz. These spectra were extrapolated to 8·87 GHz to determine the estimated flux densities. Some properties of the calibration sources are given in Table 1.

Table 1

FLUX DENSITY CALIBRATORS

(1) Parkes source No.	(2) Other cat. No.	(3) Identification	(4) Size factor	(5) Flux density S_{est}	(6) S_{meas}	(7) Ratio S_{est}/S_{meas}
0003−00*	3C 2	QSO	1·000	0·91	0·94	0·968
0023−26	MSH 10	—	1·000	2·59	2·45	1·057
0034−01	3C 15	E	1·006	1·03	1·00	1·030
0035−02	3C 17	E	1·017	1·72	1·82	0·945
0159−11	3C 57	QSO	1·000	0·90	1·00	0·900
0410−75	MSH 1	—	1·000	2·65	2·54	1·043
0521−36†	MSH 6	N	1·005	7·20	7·11	1·013
1116+12		QSO	1·000	1·32	1·33	0·992
1932−46	MSH 6	g	1·052	2·03	1·93	1·052
2121+24	3C 433	db	1·025	2·30	2·31	0·996

* Possibly a variable (see Table 3). Flux density given by Andrievskii *et al.* (1969) is in conflict with other flux density data which support a stable power-law spectrum.

† A slow variable. Value is that estimated for 1972·1.

Subsequent to the observations, corrections for differences between the set and measured coordinates of each source were applied to the flux densities from the on–off series. (These corrections were obtained graphically from the beam pattern obtained from a scan through a strong small-diameter source.) The flux densities from the two on–off series for each source were then averaged. The final flux densities were determined by multiplying these averages by a scale factor obtained from the calibration sources given in Table 1. The measured flux densities of the 10 calibrator sources are given in column 6 of Table 1. The r.m.s. scatter in the ratio of estimated to measured flux densities (column 7) is 4·8%.

The size factors (used in correcting the peak flux densities for partial resolution) have been estimated from all available data on angular structure by means of the formulae given by Shimmins and Bolton (1972*a*). Most of these data are from observations at frequencies lower than the present measurements (e.g. 408, 1425, and

2650 MHz). In the case of core–halo sources, allowances were made for changes in structure with frequency. The computed size factors for 150 of the 195 sources measured were not significantly different from unity, and in only 20 cases were the factors greater than 1·05.

IV. Estimation of Errors

In the present observations errors in flux density due to polarization, confusion, and receiver nonlinearity are negligibly small. Flux density errors arise from:

(1) uncertainties in the zenith angle correction factor,
(2) changes in atmospheric extinction,
(3) system noise and telescope tracking "noise",
(4) short-term changes in receiver sensitivity,
(5) measurement of the amplitude of the calibration signal, and
(6) uncertainties in the off-source pointing factors arising from errors in the measured coordinates of the source.

Errors from the uncertainties in the zenith angle correction factor and from changes in atmospheric extinction are estimated at 3·0%, as indicated by the scatter in the observations used to determine the curve given in Figure 1 and from the scatter in a few repeated observations of strong sources. Future repeated observations will establish the value with more certainty, this being the predominant error in the flux densities of the stronger sources.

The error due to system noise and telescope tracking "noise" has been estimated as 0·020 f.u. plus 1·5% of the flux density (r.m.s. errors). The telescope tracking error is typically 2″ to 3″ arc, which results in fluctuations in output signal when the telescope beam is not exactly on source. For sources weaker than 1·5 f.u. a typical r.m.s. scatter of 0·030 f.u. is calculated from the four amplitude changes obtained from each on–off series. For the same sources the half-differences between the measured amplitudes of the first on–off series (corrected for the off-source pointing factor) and the second on–off series have an r.m.s. scatter of 0·020 f.u. Figure 3 is a histogram of these half-differences. The error agrees well with the estimate obtained from the scatter in the individual amplitudes and indicates that the errors in the first off-source pointing correction factors do not make any significant contribution to the overall errors. For the strong sources the corresponding scatter in the half-differences between the first and second on–off series is estimated as 1·5% of the flux density. This arises principally from tracking "noise", with only a small contribution from errors in the first off-source correction factors. It should be noted from Figure 3 that the half-differences do not have a normal distribution in that there is a long tail to the distribution, approximately 15% of the sources having half-differences greater than two standard deviations and 8% of the sources having half-differences greater than three standard deviations.

Errors due to short-term changes in receiver sensitivity and in the measured amplitude of the calibration signal are estimated as 1·0% r.m.s. The scatter in the amplitude of the calibrations is 1·4%, which is due partly to short-term changes in receiver sensitivity but which to a large extent is due to errors in the measurement of the amplitude of the calibration signal. This is confirmed by the fact that the scatter in the half-differences of flux densities from the first and second on–off series is significantly less when the mean calibration amplitude is used than when the individual calibration amplitudes are applied separately to the associated on–off measurements.

Errors in the off-source pointing factors, which arise from uncertainties in the measured source coordinates, are estimated to be less than 0·7%. (It is estimated that for sources stronger than 2 f.u. the r.m.s. errors in the measured coordinates are less than 5″ arc, while for sources of 1 f.u. they are approximately 8″.)

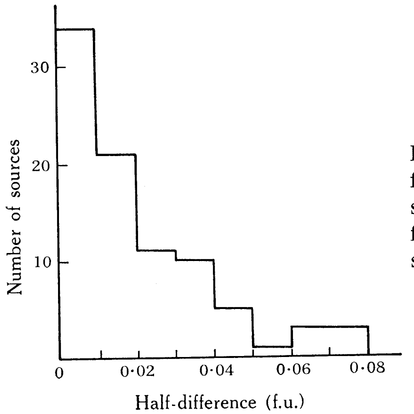

Fig. 3.—Histogram of half-differences between flux density from first on–off integration series (corrected by off-source correction factor) and that from second series, for sources with $S_{8870} \leqslant 1 \cdot 50$ f.u.

The resultant errors in the flux densities due to the sources of error discussed above are given by a standard error of $\{(0 \cdot 020)^2 + (0 \cdot 035\, S)^2\}^{\frac{1}{2}}$ f.u., where S is the flux density at 8·87 GHz. Approximately 10% of the sources show abnormally large differences between the flux densities from the declination and right ascension measurements, and these sources have been given larger estimated errors. Finally, it should be noted that for the 20 sources with size factors greater than 1·05, an additional error corresponding to 10% of the size factor has been given.

V. Notes on Table 2

Table 2 contains details of the measured sources, the flux densities at 8·87 GHz, and the estimates of errors. All flux densities are at epoch 1972·10. Additional information is:

Column 1. Parkes source number. Sources from the Parkes 2700 MHz catalogues have three digits in the declination part of their number.

Column 2. 3C, Third Cambridge catalogue (Edge *et al.* 1959); 4C, Fourth Cambridge catalogue (Pilkington and Scott 1965; Gower *et al.* 1967); MSH, catalogues of Mills *et al.* (1958, 1960, 1961).

Column 3. The measured peak flux density.

Column 4. The size factor to correct for partial resolution with the 2′·55 arc beam.

Column 5. The integrated flux density at 8·87 GHz.

Column 6. The estimated standard error in the peak flux density.

TABLE 2

8·87 GHz FLUX DENSITIES OF RADIO SOURCES

(1) Parkes source number	(2) Other catalogue numbers 3C	4C	MSH	(3) Peak flux dens. (f.u.)	(4) Size factor	(5) Flux density (f.u.)	(6) Std error (f.u.)	(7) Identification Type	Mag.	(8) Source structure*	(9) Remarks
0003−06				1·62	1·000	1·62	0·06				NRAO 5, var?
0003−00	2	−00·1	1	0·94	1·000	0·94	0·04	QSO	19·5	~7″ (MM)	Scint., NRAO 7, var?
0020−25			7	0·43	1·123	0·48	0·03	g	20	Doub., sepn. 65″, PA 129° (F2)	Scint.
0022−423				1·03	1·000	1·03	0·06	III			
0023−26			10	2·45	1·000	2·45	0·09	III		<18″×<15″ (E; FM)	
0034−01	15	−01·3	9	0·95	1·006	1·00	0·04	E	17·1	Trip., 18″×<15″ (Hd; FM)	NRAO 30
0035−02	17	−02·3	9	1·79	1·017	1·82	0·07	E	19·6	Core 20″+halo (T1)	NRAO 33
0038+09	18	09·2	11	1·04	1·035	1·08	0·06	E	18·5	41″×10″ (B; FM)	NRAO 34
0039−44			10	0·71	1·000	0·71	0·04	III		<15″ EW (FM)	
0043−42			11	1·53	1·410	2·16	0·07	E	18	Doub., sepn. 108″, PA 136° (E)	
0045−25			22	1·34	1·100	1·47	0·06	S	7·0	Core 42″ D.+halo ~300″ D. (E; F2)	NGC 253
0048−09				3·45	1·000	3·45	0·18	g	18·5		Very blue, in cluster, var.
0056−00		−00·6		1·22	1·000	1·22	0·05	QSO	17·3	<7″ (MM)	PHL 923, DA 32, var?
0106+01		01·2		3·82	1·000	3·82	0·14	QSO	18·4	<7″ (Mi)	Var.
0112−017				1·42	1·000	1·42	0·05	QSO	18·0		
0114−21			6	0·66	1·000	0·66	0·03	db	19	<18″×<15″ (E; FM)	Scint.
0116+08		08·6	2	0·83	1·000	0·83	0·04	III		<18″×<15″ (FM)	
0117−15	38		9	0·83	1·042	0·86	0·04	III		38″×<8″ (FM; B)	NRAO 67
0119+11				0·82	1·000	0·82	0·04	g	18·5	<18″×<15″ (FM)	Var?
0122−00				1·16	1·000	1·16	0·07	QSO	17·0	<7″ (MM)	Var?
0149+21				1·18	1·000	1·18	0·09	III			
0157−31			15	0·73	1·026	0·75	0·03	QSO	19	30″×<15″ (C; H; FM)	
0159−11	57		21	1·00	1·000	1·00	0·04	QSO	17·5	<7″ (MM), <1″·5 (B)	NRAO 88
0202+14		15·5		2·78	1·000	2·78	0·10	III		<0″·05 (P)	Scint., NRAO 91, var?
0202−17				1·74	1·000	1·74	0·06	QSO	19·0	Doub., <30″×<24″ (C)	Var.
0213−13·2	62		5	1·00	1·074	1·07	0·04	E	18·5	Doub., 50″ EW (F1)	NRAO 98
0229+13		13·14		1·14	1·000	1·14	0·05	QSO	18·0	<7″ (MM)	Var.
0235−19			10	0·80	1·028	0·82	0·04	IIIB		<30″×32″ (M; FM)	
0237−23				2·36	1·000	2·36	0·08	QSO	16·6	0″·002 (K)	
0240−00	71	−00·13	14	1·20	1·000	1·20	0·05	S	9·8	<21″×12″ (FM; B)	NGC 1068, NRAO 112, var?
0252−71			2	0·89	1·000	0·89	0·04			<24″ D. (E)	
0253+13				0·36	1·000	0·36	0·02	IIIA			
0302−623				1·26	1·000	1·26	0·05	QSO	18·0		
0305+03	78	03·5	3	2·54	1·150	2·92	0·10	D	14·7	Core <45″×<30″+halo 55″×80″ (F2)	NGC 1218, NRAO 124
0307+16	79	16·7		0·63	1·092	0·69	0·03	E	19	Doub., sepn. 56″ EW (M; F1)	NRAO 125

* See abbreviations of references at end of table.

TABLE 2 (*Continued*)

(1) Parkes source number	(2) Other catalogue numbers 3C	4C	MSH	(3) Peak flux dens. (f.u.)	(4) Size factor	(5) Flux density (f.u.)	(6) Std error (f.u.)	(7) Identification Type	Mag.	(8) Source structure*	(9) Remarks
0316+16		16·9		1·62	1·000	1·62	0·06	IIIB		<0″·05 (P)	Scint., CTA 21
0320+05		05·14		0·44	1·000	0·44	0·02	g	20	<18″×<15″ (FM)	Scint.
0332−403				1·80	1·000	1·80	0·07	QSO	18		
0336−01				4·39	1·000	4·39	0·15	QSO	17·5	<7″ (MM)	CTA 26, DA 110, var.
0403−13				2·20	1·000	2·20	0·08	QSO	17·1	<0″·05 (P)	Scint.
0405−12			2	1·85	1·008	1·87	0·07	QSO	14·8	Doub., sepn. 17″, PA 7° (MM)	
0409+22	108	22·8		0·59	1·000	0·59	0·03	III			NRAO 167
0410−75			1	2·54	1·000	2·54	0·09	IIIB		<24″ D. (E)	
0410+11	109	11·18		1·12	1·181	1·32	0·05	N	18·7	Doub., sepn. 78″ (M; F1)	NRAO 169
0413−21			4	1·07	1·000	1·07	0·06	QSO?	19·5	<30″×<15″ (FM)	Scint.
0420−01				1·78	1·000	1·78	0·06	QSO	18·0	<7″ (MM)	Var.
0422+00			5?	0·64	1·000	0·64	0·03	III			Var?
0428+20				1·72	1·000	1·72	0·06	IIIA		<30″ NS (C)	
0430+05	120	05·20		11·69	1·000	11·69	0·41	S	15·0	<0″·05 (P)	Scint., NRAO 182, var.
0438−43			9	3·79	1·000	3·79	0·19	g	19·5	<24″×<15″ (E; FM)	Var.
0440−00			15	1·93	1·000	1·93	0·07	QSO	19·2	<0″·05 (P)	NRAO 190, DA 145, var.
0451−28				2·05	1·000	2·05	0·07	QSO	19	<40″×<15″ (FM)	Var?
0453−20			22	1·26	1·068	1·35	0·05	E	14	48″×<15″ (E; C; FM)	
0454−46			12	2·36	1·000	2·36	0·08			<15″ EW (FM)	
0458−02		−02·19		2·09	1·000	2·09	0·07	N	20		DA 157, BSO, no UVX, var.
0459+25	133	25·16		1·62	1·000	1·62	0·06	III		Doub., sepn. 12″ EW (T2)	CTD 31, NRAO 199
0500+019				1·35	1·000	1·35	0·05	III			
0506−61			1	2·63	1·000	2·63	0·13	—			
0507+17				1·40	1·000	1·40	0·05	IIIC			Var?
0518+16	138	16·12		2·78	1·000	2·78	0·10	QSO	18·8	0″·4, PA 70° (Mi)	Scint., NRAO 205, var.
0521−36			6	7·08	1·005	7·11	0·25	N	16·8	<30″×14″ (E; FM)	Var.
0531+19				1·77	1·000	1·77	0·06	E	17·7	<24″ EW (C)	
0537−441				8·69	1·000	8·69	0·46	QSO	15		
0605−08				4·33	1·000	4·33	0·15	IIIA		<40″ NS (FM)	Var?
0607−15				1·18	1·000	1·18	0·05	III			Var.
0610+26	154	26·20		1·45	1·060	1·54	0·06	IIIA		<30″×45″, doub. (T2; M)	CTD 42, NRAO 230
0624−05	161	−05·23	4	4·09	1·012	4·14	0·15	III		20″×<15″ (FM)	Scint., NRAO 236, slow var.
0625−53			5	0·92	1·170	1·08	0·04			84″×36″ (E)	
0637−75			1	7·06	1·000	7·06	0·25	II		<18″ D. (E)	Var.
0715−25			4	0·92	1·000	0·92	0·04	IIIA		<18″×<15″ (FM; E)	
0723−008				1·92	1·000	1·92	0·07	III			DW 0723−00, var.
0727−11				4·80	1·000	4·80	0·25	III			
0735+17				1·71	1·000	1·71	0·06	III		<30″×<15″ (FM)	Scint., var.

0736+01				1·72	1·000	1·72	0·06	QSO	18·0	<7″ (MM)	Scint., var.
0742+103				2·79	1·000	2·79	0·10	III			DW 0742+10
0743−006		−00·28		1·79	1·000	1·79	0·06	QSO	18		
0744−67				1·59	1·000	1·59	0·06				
0802+21				0·55	1·000	0·55	0·03	III			
0805−07				0·99	1·000	0·99	0·04	QSO?	19		Var?
0818+17		17·44		0·41	1·000	0·41	0·03	g	19		Scint.
0820+22		22·21		1·56	1·000	1·56	0·06	QSO?	19·5		
0823+033				1·79	1·000	1·79	0·06	II			
0834−20				3·19	1·000	3·19	0·16	QSO?	18	<0″·05 (P)	Scint.
0834−19				0·91	1·000	0·91	0·04	III			
0842−75			1	0·96	1·000	0·96	0·04	III		<24″ D. (E)	
0850+14	208	14·28		0·30	1·002	0·30	0·02	QSO	17·4	Doub., sepn. 10″·5, PA 77° (MM)	Scint., NRAO 301
0851+14	208·1	14·29		0·56	1·000	0·56	0·03	III		<25″×<18″ (FM)	NRAO 303
0859−25			19	0·94	1·038	0·97	0·04	III		<35″×36″ (FM)	
0859−14			1	1·95	1·000	1·95	0·07	QSO	16·6	<7″ (MM)	Var.
0903+16	215	16·26		0·31	1·015	0·32	0·02	QSO	18·3	Trip., 25″, PA 140° (MM)	NRAO 315
0906+01		01·24		1·12	1·000	1·12	0·04	QSO	17·5		Var?
0915−11	218		4	7·87	1·050	8·25	0·28	D	14·8	Core 15″×47″, PA 37°, +halo (F2)	Hydra A, NRAO 319, halo 200″ D.
0920−39			4	2·47	1·007	2·49	0·09	III		<90″×16″ (FM)	
0939+14·0	225?	14·32		0·50	1·000	0·50	0·03	III			Scint., NRAO 332
0947+14	228	14·34		0·72	1·085	0·78	0·03	QSO	18·0	54″×<15″ (FM)	Scint., NRAO 337
1005+07	237	07·30	1	1·11	1·026	1·24	0·05	III		30″×<15″ (F1; M)	Scint., NRAO 347
1039+02		03·18	7	0·61	1·000	0·61	0·03	g	19·4	<18″×<15″ (FM)	DA 288
1040+12	245	12·37		1·04	1·000	1·04	0·04	QSO	17·2	Doub., sepn. 3″ (Hd; B; P)	Scint., NRAO 358, var?
1049+21		21·28		1·05	1·000	1·05	0·04	QSO?	19		
1055+01		01·28	10	3·26	1·000	3·26	0·12	QSO	18·3	<0″·05 (P)	Scint., DA 293, var.
1057−79				1·71	1·000	1·71	0·06				
1104−445				2·29	1·000	2·29	0·08	QSO	17·0		
1116−46				1·53	1·025	1·57	0·06	QSO?	17·0	30″×17″ (E; FM)	
1116+12		12·39		1·33	1·000	1·33	0·05	QSO	19·3	<7″ (MM)	Scint.
1127−14				4·72	1·000	4·72	0·17	QSO	16·9	<0″·05 (P)	Var?
1136−13			8	2·04	1·016	2·07	0·07	QSO	16·0	Doub., sepn. 23″, PA 120° (MM)	Scint., var?
1148−00		−00·47		1·45	1·000	1·45	0·05	QSO	17·7	0″·0019 (K)	Scint., var.
1151−34			14	1·83	1·000	1·83	0·07	QSO	18	<24″ D. (E)	Scint.
1213−17				1·55	1·000	1·55	0·06	III			Var.
1215−45			3	1·44	1·017	1·47	0·05	III		24″×<15″ (E; FM)	
1226+02	273	02·32	8	46·30	1·010	46·6	1·6	QSO	12·8	Doub., sepn. 19″ (Hd)	Scint., NRAO 400, var.
1228+12	274	12·45		41·59	1·170	48·6	1·5	E	9·9	Core 20″×40″+halo 400″ D. (F2)	M87, Virgo A, NGC 4486, NRAO 401
1229−02		−02·55		0·80	1·000	0·80	0·04	QSO	16·7	7″ (Mi)	Scint., var?
1237−10				1·08	1·000	1·08	0·04	QSO	18·2		Var?
1245−19				1·72	1·000	1·72	0·06	III		<0″·05 (P)	Scint.
1245−41			5	0·78	1·040	0·81	0·04	E	12·2	36″×23″ (E; FM)	NGC 4696

* See abbreviations of references at end of table.

TABLE 2 (*Continued*)

(1) Parkes source number	(2) Other catalogue numbers 3C	4C	MSH	(3) Peak flux dens. (f.u.)	(4) Size factor	(5) Flux density (f.u.)	(6) Std error (f.u.)	(7) Identification Type	Mag.	(8) Source structure*	(9) Remarks
1252+11				1·08	1·000	1·08	0·04	QSO	16·6	<5″ (MM)	Var.
1253−05	279	−05·55	20	14·01	1·000	14·01	0·75	QSO	17·8	<0″·025 (P)	Scint., NRAO 413, var.
1302−49			1	1·70	1·068	1·81	0·07	S	9·2	Core <30″ D. +halo (E)	NGC 4945, 40″ D. (Scans)
1306−09			2	1·44	1·017	1·46	0·06	D	18·5	<25″×24″ (FM; E)	Scint., very blue, var?
1313+07		07·32	5	0·41	1·295	0·53	0·03	D	15·5	Doub., sepn. 100″, PA 73° (F2)	Comps <30″ D.
1323−61				2·08	1·000	2·08	0·07				
1328+25·4	287	25·43		2·42	1·000	2·42	0·09	QSO	17·7	<0″·05 (P)	CTD 81, NRAO 424
1345+12		12·50		2·54	1·000	2·54	0·09	S	17·0	<18″×<15″ (FM)	Scint., var.
1351−018				0·94	1·000	0·94	0·04	III			BSO with UVX 60″ n.p.
1354−17			15	0·80	1·000	0·80	0·03	III		<60″×<60″ (Scans)	
1354+19		19·44		1·63	1·004	1·64	0·06	QSO	16·0	Doub., sepn. 13″, PA 160° (MM)	Var.
1355−41			5	0·81	1·152	0·93	0·04	QSO	16·5	84″×24″, PA 133° (E)	
1402−012				0·67	1·000	0·67	0·03	QSO	18·5		
1416+06	298	06·49	5	1·22	1·000	1·22	0·05	QSO	16·8	<6″×1″·5 (Mi; B)	Scint., NRAO 441
1421−49				4·50	1·000	4·50	0·16				
1422+20		20·33		0·44	1·000	0·44	0·02	QSO	17·5	Doub., sepn. 8″, PA 10° (MM)	
1424−41				1·31	1·000	1·31	0·05	QSO	18·0	<15″ EW (FM)	Scint.
1434+03		03·30	10	0·85	1·000	0·85	0·04	III		<18″×<15″ (FM)	Complex NS
1445−16				0·66	1·000	0·66	0·03	III			
1451−375				1·21	1·000	1·21	0·05	QSO	17·5		
1453−10			21	0·94	1·032	0·97	0·04	QSO	17·4	Doub., sepn. 33″, PA 155° (MM)	37″ sepn. (Hd), scint.
1502+036				0·81	1·000	0·81	0·04	QSO	19		Part 4C 03·31
1508−05		−05·64	5	1·98	1·000	1·98	0·07	QSO	16	<24″×<18″ (C; F1)	
1510−08			6?	3·70	1·000	3·70	0·13	QSO	16·5	<0″·05 (P)	Var.
1514+00		00·56	6	0·95	1·640	1·56	0·06	E	13·9	Trip., sepn. 232″, PA 37° (F2)	Comps 60″, 50″, 50″ D., DA 378
								QSO	18·8		
1514+07	317	07·40	5	0·41	1·026	0·42	0·02	E	14·5	30″×<15″ (FM)	NRAO 474
1514−24				1·83	1·000	1·83	0·07	E	16·2	<50″×<15″ (FM)	AP Lib, var?
1518+04·7		04·51		0·48	1·106	0·53	0·03	g	18·7	60″ (Scans)×<24″ (C)	
1532+01				1·16	1·000	1·16	0·05	III			Var?
1546+027				1·44	1·000	1·44	0·05	QSO	17·5		Var.
1549−79				2·61	1·000	2·61	0·09	III		<18″ D. (E)	
1555+001				1·66	1·000	1·66	0·06	III			DA 393, DW 1555+00
1602+01	327·1	01·48	2	0·73	1·000	0·73	0·03	IIIA		<21″×8″ (FM; B)	NRAO 491
1607+26				0·89	1·000	0·89	0·04	QSO?	19	<15″×<15″ (FM)	CTD 93
1610−77				3·27	1·000	3·27	0·12				
1616+06				0·49	1·000	0·49	0·03				DW 1616+06, var?
1622−29				1·98	1·000	1·98	0·07	IIIA		<75″×<15″ (FM)	
1635−14			13	0·42	1·000	0·42	0·02	IIIA			
1645+17	346?	17·71		0·62	1·000	0·62	0·03	QSO?	19·0	<18″×<1″·5 (FM; B	NRAO 474, var?

1730−13				4·65	1·000	4·65	0·17	IIIA		<18″×<18″ (H; FM)	NRAO 530, var.
1741−03				2·60	1·000	2·60	0·09	IIIA		<30″ EW (C)	Var?
1801+01				1·19	1·000	1·19	0·05	QSO	19·0		Var?
1814−63			1	2·40	1·000	2·40	0·09	g	18	<24″ D. (E)	Scint.
1821+10				1·29	1·000	1·29	0·05	IIIA			
1830−21				6·68	1·000	6·68	0·24	HII		<60″×<60″ (Scans)	
1904−80				1·76	1·000	1·76	0·09				
1932−46			6	1·83	1·052	1·93	0·07	g	20	42″×<18″ PA 110° (E)	Scint.
1933−400				1·10	1·000	1·10	0·04	QSO	18·0		
1934−63				2·92	1·000	2·92	0·15	g	18·4	<18″ D. (E)	Seyfert galaxy
1936−623				0·70	1·000	0·70	0·03				
1949+02	403	02·50	10	1·13	1·230	1·39	0·05	S	16·5	Doub., sepn. 76″, PA 82° (F2)	Comps 40″, 25″ D., NRAO 616
1954−388				1·90	1·000	1·90	0·07	QSO	18·5		Var?
2012+23	409	23·53		1·74	1·014	1·76	0·06	IV		22″×<15″ (FM)	NRAO 625
2052−47				1·84	1·000	1·84	0·07			<15″ EW (FM)	
2106−413				1·92	1·000	1·92	0·07	IIIB			
2121+24	433	24·54		2·26	1·025	2·31	0·12	db	18·7	30″×17″ (FM)	CTD 130, NRAO 658
2127+04				1·45	1·000	1·45	0·05	III		<18″×<15″ (H; FM)	
2128−12				1·76	1·000	1·76	0·06	QSO	16·0	<7″ (MM)	
2134+004				12·30	1·000	12·30	0·43	QSO	17	0″·0015 (K)	DA 553, PHL 61
2141−75				0·93	1·000	0·93	0·04				
2145+06		06·69		4·01	1·000	4·01	0·14	QSO	16·5	<0″·05 (P)	Var.
2203−18			1	3·30	1·000	3·30	0·12	QSO	19·5	<0″·05 (P)	Scint.
2210+01		01·69		0·64	1·000	0·64	0·03	IIIB		<18″×<15″ (FM)	DA 575
2216−03		−03·79	6	2·89	1·000	2·89	0·10	QSO	16·4	<7″ (MM)	Var?
2223−05	446	−50·92	10	4·46	1·000	4·46	0·16	QSO	18·4	<0″·05 (P)	Scint., NRAO 687, var.
2227−08				1·96	1·000	1·96	0·10	QSO	18		
2230+11		11·69		2·48	1·000	2·48	0·09	QSO	17·3	<0″·05 (P)	Scint., CTA 102, var.
2247+14		14·82		0·92	1·000	0·92	0·04	QSO	17·5	<18″×<15″ (FM)	
2251+15	454·3	15·76		13·29	1·000	13·29	0·47	QSO	16·1	<0″·025 (P)	Scint., NRAO 701, var.
2307+10		10·70?		0·88	1·000	0·88	0·04	III			
2313+03	459	03·57	5	0·68	1·000	0·68	0·03	N	18·7	<18″×6″ (FM; B)	Doub. EW (B), NRAO 709
2319+07				0·59	1·000	0·59	0·03	QSO	17·5		Var?
2324−02			11	0·61	1·221	0·74	0·03	E	18	72″ D. (C)	DA 602
2331−41			4	0·81	1·026	0·83	0·04	III		<24″×30″ (E)	Var?
2333−528				1·08	1·000	1·08	0·04				
2344+09		09·74		1·74	1·000	1·74	0·06	QSO	16·0	<7″ (MM)	Var?
2345−16				2·74	1·000	2·74	0·10	QSO	18·5	<24″×<24″ (C)	
2353−68				1·04	1·000	1·04	0·04	QSO	17·0		
2354−11				1·07	1·000	1·07	0·04	QSO	19·0	<30″×<24″ (C)	

* Abbreviations of references are:

B, Bash (1968); C, Cole, Milne, and Wall (unpublished data from Parkes interferometer); E, Ekers (1970); F1, Fomalont (1968); F2, Fomalont (1971); FM, Fomalont and Moffet (1971); H, Beverley Harris (unpublished data from Parkes interferometer); Hd, Hazard (1965) (occultation data); K, Kellermann *et al.* (1970); M, Maltby and Moffet (1962); Mi, Miley (1971); MM, Macdonald and Miley (1971); P, Palmer *et al.* (1967); Scans, data from scans at 5009 MHz (Parkes Observatory); T1, Taylor (1966) (occultation data); T2, Taylor and De Jong (1968) (occultation data).

TABLE 3

VARIABLE SOURCES

(1) PKS number	(2) Other catalogue numbers	(3) PKS/BSB	(4) Ratio of flux densities PKS/CRI	(5) PKS/M	(6) Z/DMP	(7) Identification Type	Mag.	(8) Remarks*
0003−06	NRAO 5	1·34, 1·44	0·98:					Var?
0003−00	3C 2, 4C−00·1, NRAO 7		0·65			QSO	19·5	Optical var. (SVW)
0048−09			1·44	3·3, 1·1		g	18·5	Known var. (S)
0056−00	4C−00·6, PHL 923, DA 32		1·24:			QSO	17·3	Var? (W)
0106+01	4C 01·2		1·16:			QSO	18·4	Known var. (K; M; H; PKS)
0119+11		0·62				g	18·5	Var? (B)
0122−00			0·70, 0·67			QSO	17·0	Var?
0202+14	4C 15·5, NRAO 91		1·36			QSO	17·5	Var?
0202−17			0·90:			QSO	19·0	Known var. (K)
0229+13	4C 13·14	1·30, 1·05	1·37			QSO	18·0	Known var. (B)
0240−00	3C 71, 4C−00·13, NGC 1068		0·70	0·77	1·10:	S	9·8	Var? at mm wavelengths (EF)
0336−01	CTA 26, DA 110		1·74			QSO	17·5	Known var. (K; H; PKS)
0420−01			0·83			QSO	18·0	Known var. (W)
0422+00			0·59					Var? (W)
0430+05	3C 120, 4C 05·20		0·91			S	15·0	Known var. (K; M; H)
0438−43	MSH 9					g	19·5	Known var. (H)
0440−00	NRAO 190, DA 145		0·81			QSO	19·2	Known var. (K; H)
0451−28						QSO	19	Var? (PKS)
0458−02	4C−02·19, DA 157		1·22:			N	20	Known var. (W)
0507+17		1·87						Var?
0518+16	3C 138, 4C 16·12		0·82		0·84	QSO	18·8	Known var. (M)
0521−36	MSH 6		0·99:			N	16·8	Known var. (H)
0605−08			1·80					Var?
0607−15			0·54					Known var. (K)
0624−05	3C 161, 4C−05·23		1·14:					Slow var. (H)
0637−75	MSH 1							Known var. (H)
0723−008	DW 0723−00			0·68, 1·11				Known var. (BS)
0735+17			0·91:					Known var. (K; M)
0736+01			1·29			QSO	18·0	Known var. (K; PKS)
0805−07		1·06:	0·89:			QSO?	19·0	Var? (B)
0859−14	MSH 1		0·88:			QSO	16·6	Known var. (K)
0906+01	4C 01·24	1·81	0·66			QSO	17·5	Var?
1040+12	3C 245, 4C 12·37				1·92	QSO	17·2	Var?
1055+01	4C 01·28, DA 293, MSH 10		1·39			QSO	18·3	Known var. (K; PKS)

1127−14		0·77	0·87			QSO	16·9	Var?
1136−13	MSH 8		1·58			QSO	16·0	Var?
1148−00	4C−00·47		0·77			QSO	17·7	Known var. (K; PKS)
1213−17		0·97:						Known var. (B)
1226+02	3C 273, 4C 02·32		1·24		1·02:	QSO	12·8	Known var. (D; K; M; PKS)
1229−02	4C−02·55	0·77	1·14:			QSO	16·7	Var?
1237−10		0·96:	1·05:			QSO	18·2	Var? (B)
1252+11			1·10:			QSO	16·6	(PKS)
1253−05	3C 279, 4C−05·55		0·71			QSO	17·8	Known var. (K; M; PKS)
1306−09	MSH 2		0·64			D	18·5	Var?
1345+12	4C 12·50		1·07:			S	17·0	Known var. (KPT)
1354+19	4C 19·44		1·10:			QSO	16·0	Known var. (M)
1510−08			0·90			QSO	16·5	Known var. (K; M; H; PKS)
1514−24	AP Lib		0·76			E	16·2	Known optical var.
1532+01		0·77						Var?
1546+027				0·62, 1·37		QSO	17·5	Known var. (BS)
1616+06	DW 1616+06	0·61	0·34					Var?
1645+17	4C 17·71, NRAO 474		0·50			QSO?	19·0	Var?
1730−13	NRAO 530		1·33					Known var. (K; M)
1741−03						IIIA		Var? (W)
1801+01		1·61				QSO	19·0	Var?
1954−388								Var? (PKS)
2145+06	4C 06·69		0·91:			QSO	16·5	Known var. (M)
2216−03	4C−03·79		1·45			QSO	16·4	Var?
2223−05	3C 446		0·92:			QSO	18·4	Known var. (K; M)
2230+11	CTA 102		0·75			QSO	17·3	Known var. (M)
2251+15	3C 454·3		0·54		0·61	QSO	16·1	Known var. (K; M; H)
2319+07		1·44				QSO	17·5	Var?
2331−41	MSH 4					III		Var? (PKS)
2344+09	4C 09·74	1·43	1·29			QSO	16·0	Var?

* Abbreviations of references are:

B, Bell *et al.* (1971); BS, Brandie and Stull (1971); D, Dent (1965); EF, Epstein and Fogarty (1969); H, Harris (1969); K, Kellermann and Pauliny-Toth (1968); KPT, Kellermann *et al.* (1968); M, Medd *et al.* (1968); PKS, unpublished data from Parkes Observatory; S, Stull (1971); SVW, Sandage *et al.* (1965); W, Wall (1972).

Column 7. Optical identification or field class for the source where known. These data are mainly drawn from published or unpublished identification work of the Parkes Observatory. The following abbreviations apply: QSO, quasi-stellar object; QSO ?, possible quasi-stellar object; S, E, D, db, and N, galaxies with these optical classifications; g, galaxy too faint to classify from the Palomar Sky Atlas; II, field contains several faint galaxies within positional errors; III, a few stars of normal colour; IIIA, as for III, with some obscuration possibly present; IIIB, a blank field; IIIC, a very crowded star field; IV, an obscured field; HII, an ionized hydrogen region.

Column 8. Abbreviations used are: doub., a two-component source; sepn., angular separation; PA, position angle; trip., a three-component source; NS, north–south; EW, east–west; D., diameter. Where two angular sizes are given, the north–south size is given first, followed by the east–west size.

Column 9. Remarks, including other catalogue numbers not given in column 2. Abbreviations (in addition to those given above for column 8) used are: BSO, blue stellar object; comps, components; CTA, Caltech list A of Harris and Roberts (1960); CTD, Caltech list D of Kellermann and Read (1965); DA, catalogue of Galt and Kennedy (1968); DW, catalogue of Davis (1967); M, Messier catalogue; NGC, New General catalogue; n.p., north preceding; NRAO, catalogue of Pauliny-Toth *et al.* (1966); PHL, Palomar Haro Luyten (Haro and Luyten 1962); scint., source shows interplanetary scintillation; UVX, ultraviolet excess; var., source is known to vary at centimetre wavelengths; var ?, source is thought to vary at centimetre wavelengths.

VI. Comparison with Other Results

(*a*) *Flux Density Scales and Error Estimates*

In order to compare the present measurements with those of Bell *et al.* (1971) at 6·63 and 10·7 GHz, a flux density at 8·87 GHz has been estimated by interpolation for each source in common. A plot of these flux densities against the present observations indicated that the flux density scales are the same to within the statistical uncertainty. Many of the sources common to the two lists are variable in flux density at centimetre wavelengths. The scatter in the plot reflects these variations together with any errors introduced by the interpolation procedure, and thus cannot be used to verify error estimates.

When the 8·55 GHz flux densities from the Crimean Astrophysical Observatory (Andrievskii *et al.* 1969; Gorshkov *et al.* 1970) are plotted against the present observations, it is clear that there is a significant difference between the flux density scales. If the small difference in frequency is taken into account by means of a representative spectral index, the 8·55 GHz flux densities appear to be scaled about 14% lower than the present measurements. The scatter in the plot cannot be used to verify the error analysis of Section IV because the errors in the 8·55 GHz flux densities are considerably larger than those in the flux densities presented here.

Stull (1971) has observed 60 radio galaxies from the Parkes catalogues at 8·0 GHz. There are six sources in common for which the 8·0 GHz flux densities are greater than 1 f.u. and believed not to vary. The mean ratio of 8·87 GHz flux density to 8·0 GHz flux density is $0 \cdot 967 \pm 0 \cdot 015$. A ratio of 0·92 is expected on the basis of the frequency difference and a representative spectral index of 0·8. Consequently the scale used by Stull appears to be about 5% higher than that adopted here. The error estimates for the two sets of observations are comparable and the r.m.s. scatter of 3·6% in the flux density ratios for the six sources is in good agreement with these estimates.

(*b*) *Variations in Flux Density*

Table 3 is a list of the sources in the present sample which are either known or thought to vary in flux density at centimetre wavelengths. The list comprises all sources labelled "var." or "var?" in column 9 of Table 2. For a number of sources a comparison has been made between the present observations and those by other observers at earlier epochs, and "var?" in these cases indicates that the source probably varies in flux density. Several sources suggested by other observers as being variable at centimetre wavelengths have been included, although the present observations do not necessarily support these suggestions.

Columns 3, 4, 5, and 6 of Table 3 contain the ratios of flux densities, indicated by the abbreviations (for other abbreviations see Section V.): PKS, present (8·87 GHz) observations; BSB, 6·63 and 10·7 GHz observations at Algonquin Radio Observatory (Bell *et al.* 1971) interpolated for estimates of 8·87 GHz flux densities; CRI, 8·55 GHz observations at the Crimean Astrophysical Observatory (Andrievskii *et al.* 1969; Gorshkov *et al.* 1970); M, 8·0 GHz observations at the University of Michigan Observatory (Brandie and Stull 1971; Stull 1971); Z, 10·69 GHz observations at Bochum (Zimmermann 1970); DMP, 10·63 GHz observations at Algonquin Radio Observatory (Doherty *et al.* 1969).

The ratios have been adjusted to remove the effects of the different flux density scales noted above. A colon following an entry in columns 3–6 indicates that the entry as it stands does not imply flux density variations. No reference in column 8 indicates that variations in the flux density of the source have not been suggested previously. It is clear that repeated observations for such sources are required to establish variations with certainty, as comparisons of single flux density measurements from different observatories can be misleading.

The apparent variations in PKS 0240−00 (3C 71; NGC 1068) are of particular interest. The source is known to be very luminous at infrared wavelengths (Kleinman and Low 1970), and some observers have suggested variations in flux density at millimetre wavelengths (Epstein and Fogarty 1968; Rather 1970; Fogerty *et al.* 1971). The radio spectrum (see e.g. Kellermann and Pauliny-Toth 1971) does not suggest the presence of compact components from which variations in flux density might be anticipated.

VII. Conclusions

We have demonstrated a satisfactory technique for measuring the flux densities of small-diameter sources with a relatively narrow beam under conditions of low signal to noise ratio. Comparison with measurements from other observations indicates that the flux scale at 8·87 GHz is satisfactory, and suggests variation in the flux density at this frequency for at least 30% of the sources in the sample. The use of a stronger calibration signal would reduce the error due to system noise in its measurement, and determination of the source position with integrations at $\pm 1/4$ beamwidth prior to the main on–off cycle could reduce the errors due to telescope pointing.

VIII. Acknowledgments

We thank the receiver group of the Division of Radiophysics, CSIRO, for construction and maintenance of the receiver, Mr. J. G. Bolton for discussions on and suggested modifications to the observational technique, and Mr. P. W. Butler for assistance with the observations.

IX. References

Andrievskii, A. E., *et al.* (1969).—*Astr. Tsirk. Byuro astr. Soobshch* No. 494, 1.
Bash, F. N. (1968).—*Astrophys. J. Suppl. Ser.* **16**, 373.
Bell, M. B., Seaquist, E. R., and Braun, L. D. (1971).—*Astr. J.* **76**, 524.
Brandie, G. W., and Stull, M. A. (1971).—*Nature* **231**, 149.
Davis, M. M. (1967).—*Bull. astr. Insts Neth.* **19**, 201.
Dent, W. A. (1965).—*Science, N.Y.* **148**, 1458.
Doherty, L. H., MacLeod, J. M., and Purton, C. R. (1969).—*Astr. J.* **74**, 827.
Edge, D. O., Shakeshaft, J. R., McAdam, W. B., Baldwin, J. E., and Archer, S. (1959).—*Mem. R. astr. Soc.* **68**, 37.
Ekers, Jennifer A. (Ed.) (1969).—*Aust. J. Phys. astrophys. Suppl.* No. 7.
Ekers, R. D. (1970).—*Aust. J. Phys.* **23**, 217.
Epstein, E. E., and Fogarty, W. G. (1968).—*Astr. J.* **73**, 873.
Fogarty, W. G., Epstein, E. E., Montgomery, J. M., and Dworetsky, M. M. (1971).—*Astr. J.* **76**, 537.
Fomalont, E. B. (1968).—*Astrophys. J. Suppl. Ser.* **15**, 203.
Fomalont, E. B. (1971).—*Astr. J.* **76**, 513.
Fomalont, E. B., and Moffet, A. T. (1971).—*Astr. J.* **76**, 5.
Galt, J. A., and Kennedy, J. E. D. (1968).—*Astr. J.* **73**, 135.
Gorshkov, A. G., *et al.* (1970).—*Astr. Tsirk. Byuro astr. Soobshch* No. 545, 1.
Gower, J. F. R., Scott, P. F., and Wills, D. (1967).—*Mem. R. astr. Soc.* **71**, 49.
Haro, G., and Luyten, W. J. (1962).—*Boln Observs Tonantzintla Tacubaya* **3**, 37.
Harris, Beverley J. (1969).—Ph.D. Thesis, Australian National University.
Harris, D. E., and Roberts, J. A. (1960).—*Publs astr. Soc. Pacif.* **72**, 237.
Hazard, C. (1965).—*In* "Quasi-stellar Sources and Gravitational Collapse". (Eds. I. Robinson, A. Schild, and E. L. Shucking.) p. 135. (Univ. Chicago Press.)
Kellermann, K. I., *et al.* (1970).—*Astrophys. J.* **161**, 803.
Kellermann, K. I., and Pauliny-Toth, I. I. K. (1968).—*Astrophys. J.* **152**, 639.
Kellermann, K. I., and Pauliny-Toth, I. I. K. (1971).—*Astrophys. Lett.* **8**, 153.
Kellermann, K. I., Pauliny-Toth, I. I. K., and Tyler, W. C. (1968).—*Astr. J.* **73**, 298.
Kellermann, K. I., and Read, R. B. (1965).—*Publs Owens Valley Radio Observ.* **1**, No. 2.
Kleinman, D. E., and Low, F. J. (1970).—*Astrophys. J.* **159**, L165.
Macdonald, G. H., and Miley, G. K. (1971).—*Astrophys. J.* **164**, 237.
Maltby, D., and Moffet, A. T. (1962).—*Astrophys. J. Suppl. Ser.* **7**, 141.
Medd, W. J., Locke, J. L., Andrew, B. H., and Van den Bergh, S. (1968).—*Astr. J.* **73**, 293.
Miley, G. K. (1971).—*Mon. Not. R. astr. Soc.* **152**, 477.
Mills, B. Y., Slee, O. B., and Hill, E. R. (1958).—*Aust. J. Phys.* **11**, 360.
Mills, B. Y., Slee, O. B., and Hill, E. R. (1960).—*Aust. J. Phys.* **13**, 676.
Mills, B. Y., Slee, O. B., and Hill, E. R. (1961).—*Aust. J. Phys.* **14**, 497.
Palmer, H. P., *et al.* (1967).—*Nature* **213**, 789.
Pauliny-Toth, I. I. K., Wade, G. M., and Heeschen, D. S. (1966).—*Astrophys. J. Suppl. Ser.* **13**, 65.
Pilkington, J. D. H., and Scott, D. F. (1965).—*Mem. R. astr. Soc.* **69**, 183.
Rather, J. D. G. (1970).—*Bull. Am. astr. Soc.* **2**, 339.

SANDAGE, A., VÉRON, P., and WYNDHAM, J. D. (1965).—*Astrophys. J.* **142**, 1307.
SHIMMINS, A. J. (1971).—*Aust. J. Phys. astrophys. Suppl.* No. 21.
SHIMMINS, A. J., and BOLTON, J. G. (1972*a*).—*Aust. J. Phys. astrophys. Suppl.* No. 23.
SHIMMINS, A. J., and BOLTON, J. G. (1972*b*).—*Aust. J. Phys. astrophys. Suppl.* No. 26.
STULL, M. A. (1971).—*Astr. J.* **76**, 1.
TAYLOR, J. H. (1966).—*Astrophys. J.* **146**, 646.
TAYLOR, J. H., and DE JONG, M. L. (1968).—*Astrophys. J.* **151**, 33.
THOMAS, B. MACA. (1970).—*Electron. Lett.* **6**, 460.
WALL, J. V. (1972).—*Aust. J. Phys. astrophys. Suppl.* No. 24.
WALL, J. V., SHIMMINS, A. J., and MERKELIJN, J. K. (1971).—*Aust. J. Phys. astrophys. Suppl.* No. 19.
ZIMMERMANN, P. (1970).—*Beitr. Radioastron.* **1**(6), 161.